EFFECTS OF COMPRESSION PRECRACKING ON SUBSEQUENT CRACK GROWTH

James, M.A.[1], Forth, S.C.[2], Johnston, W.M.[3], Newman, J.A.[4] and Everett, R.A.[4]
[1] National Institute of Aerospace
[2] NASA Langley Research Centre
[3] Lockheed Martin Corporation
[4] U.S. Army Research Laboratory

2 West Reid Street, MS 188E
Hampton, VA 23681 USA
m.a.james@larc.nasa.gov

Abstract

Compression precracking (CPC) has seen renewed interest as a possible alternative procedure for generating fatigue crack growth threshold data with minimal load history effects. However, recent testing confirms results from the literature that compression precracking does induce load history effects through residual stresses that influence subsequent fatigue crack growth test data. Using the CPC method, specimens are precracked with both maximum and minimum compressive loads. Compressive yielding occurs at the crack-starter notch, resulting in a local tensile residual stress field through which the fatigue crack must propagate. Although the tensile residual stress field contributes to the driving force for precracking, it also introduces the possibility of history effects that may affect subsequent fatigue crack growth. The tensile residual stress field elevates the local driving force at the crack tip, promoting higher crack growth rates than would be expected from the applied loading. This paper presents three-dimensional finite element results and experimental data for compact tension specimens that characterize the load history effects induced by compression precracking.

Introduction

Industry and regulatory agencies are developing damage tolerance methodologies for high-cycle fatigue components, such as the transmission system of a helicopter. The damage tolerance methodologies rely on fatigue crack growth (FCG) rate data to predict service life and inspection intervals. In the case of high-cycle fatigue, where many thousands of loading cycles are applied per flight hour, accurate FCG threshold data are essential because large numbers of cycles can accumulate in a very short time, causing significant crack growth even for cracks with a driving force very near the material threshold.

Fatigue crack growth data are typically generated using a load reduction procedure, where the driving force is methodically reduced to a threshold while monitoring the crack growth rates. ASTM "Standard Test method for Measurement of Fatigue Crack Growth Rates," (E647) contains two load reduction procedures for generating the FCG data: the constant K_{max} procedure and the constant load ratio procedure. The constant K_{max} procedure is not applicable for generating low load ratio threshold data and will not be discussed. The constant load ratio procedure holds the ratio of minimum to maximum load constant as the driving force is reduced to threshold. Recent experimental data and analytical results indicate that the constant load ratio procedure can produce non-conservative, high FCG thresholds [1] that could lead to the unsafe design of structures that experience high-cycle fatigue loading. Possible causes for these high thresholds are load history effects caused by the test procedure [1] and specimen configuration effects [2,3]. For example, high precracking loads can cause remote crack closure, resulting in a plasticity-induced crack-tip shielding effect that reduces the crack driving force.

Forth, *et. al.* [4], proposed using compression precracking (CPC) followed by constant load amplitude testing to generate FCG data, thus using a procedure that does not contain a load reduction component. During compression precracking, both maximum and minimum loads are compressive. The compressive loading causes yielding at the notch, which results in a tensile residual stress field [5, 6]. The cyclic nature of the compressive loading leads to crack formation in the residual stress field and drives cracking through the residual stress field until the residual stresses relax and the crack arrests [5, 7– 10]. After precracking, the constant load amplitude testing allows the crack to grow using a monotonically increasing driving force starting at near threshold growth rates. Recent test results on single edge notch bend specimens indicate that the residual stress field affects crack growth rates during the test following compression precracking [9].

Other factors such as K_{max} effects and closure development can affect crack growth rates following compression precracking. Tabernig and Pippan [8, 9, 11 – 14] have extensively studied transient effects for crack growth that begins with a fully open crack (created using either CPC or another technique). They have expended significant effort to exclude or minimize residual stress effects by annealing specimens after compression precracking and by creating extraordinarily sharp cracks. Their experimental results showed that cracks that initially grew at ΔK values below the threshold eventually arrested, and for ΔK values above the threshold cracks eventually achieved steady state growth rates consistent with baseline crack growth rate data.

The objective of this study was to further the understanding of the effects of the precracking induced residual stress state on the subsequent fatigue crack growth rate data. This understanding may lead to guidelines for using CPC to generate fatigue crack growth threshold data. Elastic-plastic finite element analyses with crack growth for a compact tension specimen, was used to model the compression precracking process and to estimate the residual stress effects. Experimental procedures for a compact tension specimen were used to quantify the amount of crack growth necessary to minimize the residual stress effects under constant ΔK loading.

Finite element analyses

The compression precracking fatigue crack growth process was modelled using the finite element code WARP3D [15, 16]. Analyses were performed for compact tension, C(T), specimens with thickness, B = 6.35 mm, width of W = 76.2 mm, notch length of a_{notch} = 19.1 mm, and notch root radius of 0.191 mm. Further details of the modelling can be found in James, *et al* [17]. Several compression precracking load magnitudes were analyzed to asses the size and shape of the compressive plastic zone and to asses the effects of the plastic zone on crack tip driving force. Figure 1 is a contour plot of von Mises stresses on the crack plane at the minimum load (P_{min} = -10 kN, K_{CPC} = -28.2 MPa$\sqrt{m}$, the stress intensities presented herein assume that the notch is a crack) prior to crack initiation. Also included are lines showing the shape of the yielded region for four other lower load magnitudes. The table in Figure 1 shows load magnitudes, stress-intensity and normalized stress-intensity for each of the five yield zones noted in Figure 1. At low load magnitudes (Cases 1 and 2) the plastic zone is essentially uniform through the thickness. As the load magnitude increases, plasticity develops more rapidly at the surface, as indicated by the extended plastic zone size just below the surface in Figure 1. As the plastic zone develops, the stress triaxiality (constraint) is limited by the yielded material (commonly called constraint loss). Newman [18] characterized average constraint loss in terms of the normalized stress-intensity factor, where $K/(\sigma_o\sqrt{B}) \rightarrow 1$ represents full constraint loss. The table in Figure 1 shows that at the highest load magnitude there is near full constraint loss based on the Newman criterion.

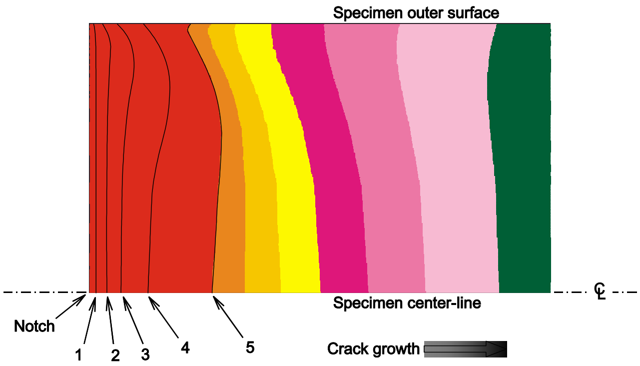

Case	P_{min}	K_{min}	$K_{min}/(\sigma_o\sqrt{B})$
1	2.73	7.69	0.25
2	4.55	12.82	0.42
3	6.37	17.94	0.58
4	8.19	23.07	0.75
5	10.00	28.20	0.92

FIGURE 1. Von Mises stresses showing plastic zone size and shape on the crack plane for load level 5 and plastic zone size for four lower compressive load levels (see side table).

An essential component of fatigue crack growth testing is that the applied K_{max} be known. ASTM E647 places tolerances on measured quantities (load, 2%; crack length, 0.1 mm or 0.002W, whichever is greater; etc.). However the standard does not place tolerances on calculated quantities such as K_{max}. Based on the ASTM E647 tolerances on load and crack length, it is not unreasonable to set a tolerance on K_{max} of 5%. Based on this level of acceptable difference, it is feasible to determine the point where the K_{max} value with residual stress effects included (K_{tip}) is within acceptable limits of the applied value ($K_{max\text{-}applied}$). Figure 2 shows normalized crack growth ($\Delta a/r_p$) necessary for a 5% difference between K_{tip} and applied K_{max}.

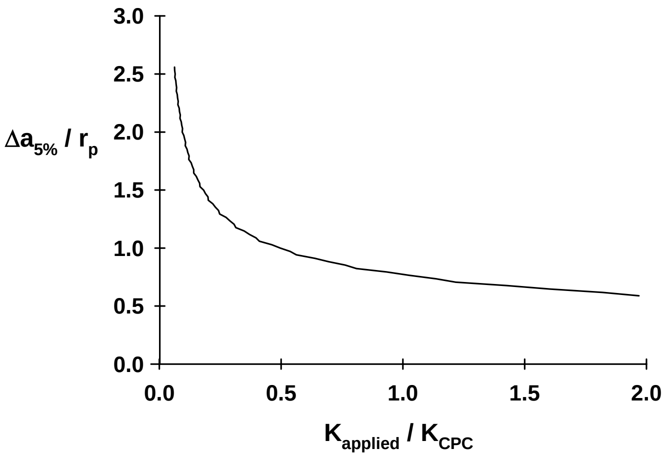

FIGURE 2. Amount of crack growth necessary to reduce the difference between $K_{max\text{-}applied}$ and K_{tip} to within 5% nondimensionalized to K_{CPC}.

The normalized crack growth is a function of crack growth, Δa, divided by the calculated plastic zone size from compression precracking, r_p. The normalized stress-intensity is a function of the applied K and the compression precracking K level. As the applied tensile load increases, for a fixed compressive precracking loading, the effect of the residual stresses diminish. Conversely, as the compressive precracking load increases, and the subsequent tensile loading remains constant, the effect of the residual stresses intensify. Finally, at low values of driving force, which are necessary for threshold determination, the residual stress effects of all but the lowest levels of compression load are significant.

Experimental Results

This section first describes the experimental results that were used to verify the finite element analyses. Then experimental results are presented to compare the effect that the traditional tensile and compressive precracking procedures have on crack growth rate data. Figure 3 is a plot of experimental crack growth versus cycle count results for a loading case similar to the finite element analysis of case 5 presented in Figure 1. The C(T) specimens dimensions are W = 76.2 mm and B = 12.7 mm. The specimens were compression precracked at K_{CPC} = -38.5 MPa√m and R = 20 for approximately 400 cycles at room temperature, which resulted in approximately 0.5 mm of precrack growth. Then tensile loading was applied at constant ΔK = 3.33 MPa√m, R = 0.1. Under constant ΔK loading, crack growth rates are expected to be a constant steady-state value, which is a straight line on a plot of crack length versus cycles. Figure 3 shows the results of two tests run with these conditions. (Note that the second test ended prematurely at about 500,000 cycles due to a computer problem.) The final seven data points of the first test were fit with a straight line to determine the average crack growth rate (slope of the data) as 7.6E-5 mm/cycle. The extended line shows that the initial growth rates are higher than steady state (data has a steeper slope), but gradually decrease. Here, steady state crack growth occurs at about Δa = 4.3 mm, which is slightly more than two times the FEA estimated plastic zone size for this precrack condition. Thus these test results agree quite well with the analysis results presented in Figure 2, where crack growth of about twice the plastic zone size is required to reduce the difference in total K_{tip} to about 5%.

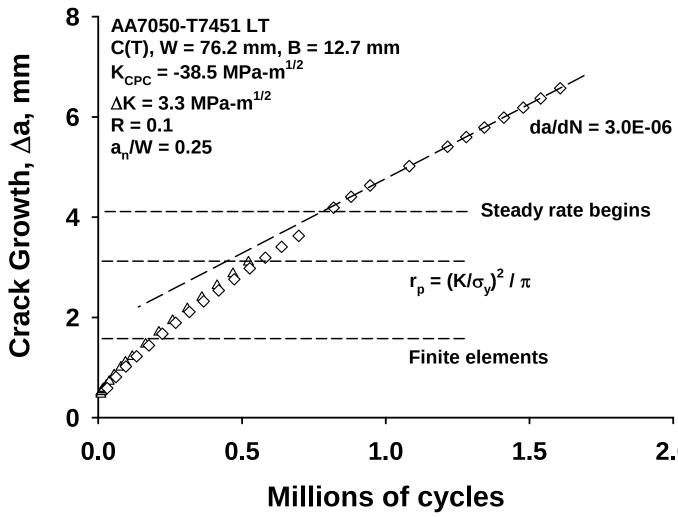

FIGURE 3. Crack length versus cycles showing the elevated growth rates caused by the residual stress field [17].

Figure 4 is a plot of growth rate data that compares standard tensile precracking with the effects of compression precracking (CPC). The figure includes baseline data for reference purposes and includes data for crack growth parallel (LT) and transverse (TL) to the material rolling direction. The baseline data, which includes a constant K_{max} test and a constant R = 0.7 test, form the basis for a ΔK_{eff} relationship used by Newman [1]. The ΔK_{eff} relationship models the crack as fully open, and all load ratio effects are modelled using plasticity-induced closure [1]. The dashed line shows the predicted R = 0.1 curve based on plasticity induced closure. The open symbols are data for material in the LT orientation, and the dotted symbols are data for material in the TL orientation. The dotted triangle and dotted circle are data for compression precracking specimens that were run for significant constant ΔK to establish steady state, then had a standard load reduction test from the constant ΔK end point. The dotted square data are for traditional precracking.

The results show that for this material there is essentially no difference in crack growth rates between data from traditional precracking and from compression precracking, as long as the CPC residual stress effects have been minimized, and as long as the testing procedure is the same. That is, the only major difference between the dotted traditional precracking data and the dotted compression precracking data is the precracking procedure. The open squares are data started at a higher initial ΔK level, and these data appear to show a higher threshold that may be attributable to starting level. Note that the initial growth rates are nearly an order of magnitude greater than suggested by ASTM E647. More testing is required to characterize a relationship between starting level and threshold.

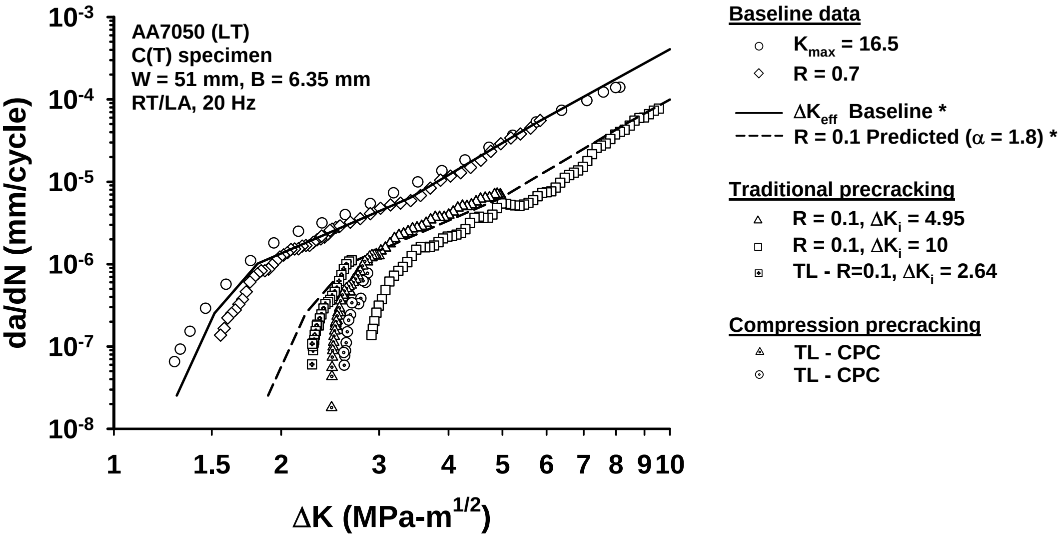

FIGURE 4. Crack growth rate data [17]. (*Provided by J. Newman, Miss. State U.).

Discussion

The results presented in Figures 1 through 3 show that compression precracking does introduce residual stresses. These residual stresses can cause crack growth rates that are significantly greater than the expected steady-state value for the applied loads. One might think that the effects of residual stresses would be limited to the yielded material in the plastic zone, because some stress relief is expected to occur as the crack propagates through this region. However, a significant volume of material yields above the crack plane, and this yielded material continues to influence crack growth well beyond the edge of the plastic zone. The experimental constant ΔK results show that the residual stresses affect the crack-tip driving force until the crack propagates two to three times the notch-tip analysis plastic zone size.

Summary

Compression precracking provides a means of creating a fully open sharp crack. The absence of crack closure allows subsequent crack growth at very low applied ΔK levels significantly below those normally possible from standard tensile precracking. This is possible because the compressive loading yields the crack starter notch, creating a tensile residual stress field at the notch root. However, the residual stresses caused by the compression precracking continue to affect crack growth rates even after the fatigue crack propagates beyond the edge of the compressive plastic zone. In addition, results from the literature show that steady-state crack closure can take a significant amount of crack growth to develop (on the order of 5 mm). Because of the combined the effects of residual stresses and closure development, crack growth rate data generated after compression precracking must be interpreted carefully. Both of these effects, decreasing residual stresses and increasing crack closure, likely contributed to the transient decreasing growth rates observed under constant ΔK loading. Local closure measurements were not performed, so it is unclear which effect dominated the observed results. In this study, more than two times the analysis plastic zone size is needed to ensure steady state growth rate conditions. However, the duration of the transient is dependent on the compressive loading level, the subsequent tensile loading level, and on material characteristics such as yield behaviour. Constant ΔK testing following compression precracking demonstrates when residual stress effects are no longer significant and ensures consistent growth rates.

References

1. Newman, J.C., Jr., *Fatigue Crack Growth Thresholds, Endurance Limits, and Design*, ASTM Press, 2000, 227-251.
2. Garr, K.R. and Hresko, G.C., III, *Fatigue Crack Growth Thresholds, Endurance Limits, and Design,* ASTM Press, 2000, 155-174.
3. Haakon, O. L. and Stephens, R. R*, Fatigue Crack Growth Thresholds, Endurance Limits, and Design*, ASTM Press, 2000, 175-191.
4. Forth, S.C., Newman, J.C., Jr., and Forman, R.G., *Int. Journal of Fatigue*, **25**, 2003.
5. Hubbard, R. P., *J. Basic Engineering*, Trans ASME, 1969, 625-631.
6. Hill, R., *The Mathematical Theory of Plasticity*, Oxford University Press, London, 1950.
7. Suresh, S., *Engineering Fracture Mechanics*, vol. **21**, 452-463, 1985.
8. Tabernig, B. and Pippan, R., In *Proceedings Fatigue-99*, 1999, 1477-1482.
9. Tabernig, B. and Pippan, R., *Engineering Fracture Mechanics*, vol. **69**, 899-907, 2002.
10. Aswath, P. B., Suresh, S., Holm, D. K., and Blom A. F., *Journal of Engineering Materials and Technology*, vol. **110**, 278-285, 1988.
11. R. Pippan, M. Berger, and H.P. Stuwe, *Metallurgical Transactions*, vol. **18A**, 429-435, 1987.
12. Pippan, R., Stüwe, H.P., and Galos, K., *Int. Journal of Fatigue*, vol. **16**, 579-582, 1994.
13. Pippan, R., Plochl, L., Dlanner, F., and Stuwe, H.P., *Journal of Testing and Evaluation*, vol. **22**, 98-103, 1994.
14. Tabernig, B., Powell, P., and Pippan, R., *Fatigue Crack Growth Thresholds, Endurance Limits, and Design*, ASTM Press, 2000, 96-108.
15. Gullerud, A. S., Koppenhoefer, Roy, A., Roychowdhury, S., Walters, M., and Dodds, R. H., Jr., *WARP3D -- Release 14.0 users manual*, 2002.
16. Gullerud, A. S., Dodds, R. H., Jr., Hampton, R. W., Dawicke, D. S., *Engineering Fracture Mechanics,* vol. **63**, 347-374, 1999.
17. James, M. A., Forth, S. C., and Newman, J. A., *Fatigue and Fracture Mechanics: 34th Volume*, ASTM Press, 2004
18. Newman, J. C., Jr., Crews, J. H., Jr., and Bigelow, C. A., *Constraint Effects in Fracture: Theory and Application*s, ASTM Press, 1995, 21-42.